2014 IEEE International Conference on Robotics & Automation (ICRA)
Hong Kong Convention and Exhibition Center
May 31 - June 7, 2014. Hong Kong, China

Compliance Control for Standing Maintenance of Humanoid Robots under Unknown External Disturbances*

Yaliang Wang, Rong Xiong, Qiuguo Zhu and Jian Chu[1]

Abstract— **For stable motions of position controlled humanoid robots, ZMP (Zero Moment Point) control is widely adopted, but needs to be integrated with other controllers due to its relatively slow response and the execution error of robots. While CoM (Center of Mass) control is much more directly than ZMP feedback control in the view of rejecting unknown external disturbance. In the meanwhile, we hope the position-based humanoid robot can have the whole body compliance in standing maintenance. So we proposes a CoM compliance controller to achieve stable standing of position controlled humanoid robot under unknown disturbance. The controller uses the concept of force control and integrates virtual model control with admittance control, where an AMPM (Angular Momentum including inverted Pendulum Model)-based virtual model with variable gain is designed to not only generate desired recovery force but also take the GRF (Grand Reaction Force) constraints into account, while an admittance controller is employed to transform the desired force to expected CoM position and body attitude. The experiments were conducted on the humanoid robot 'Kong' by exerting external force disturbance and changing the slope of the ground to demonstrate the effectiveness and robustness of our method.**

I. INTRODUCTION

Due to the intrinsic unstable feature, bipedal humanoid robots are easy to fall over and get damaged, especially when different disturbances such as unknown external force and uneven ground exist. The ability to keep balance and remain stable thus is of great importance to humanoid robots and attracts a lot of attention in related research fields. Various methods have been proposed to improve the stability of the robot under various task conditions, such as standing [1][2][3], walking [4][5][6], running [7][8], jumping [9], fast manipulating [10], etc. This paper focuses on how to keep humanoid robots standing stable when they are subject to unknown external interference.

There are two categories of adjusting strategies. One is adjusting the body configuration of the humanoid robot while keeping the foot of the robot fixed to the original location [2][3], which is called standing maintenance in this paper. Another is stepping out to gain a larger support polygon [11]. For most conditions when both strategies are sufficient, the former is always preferred over the latter. First, the balance problem for standing maintenance is simpler than that of stepping out, because there is no need to consider the questions of supporting leg selection and switch. Second, stepping out requires larger instantaneous torque on the swing leg. Finally, standing maintenance is a natural preference for human in most situations. Of course, when disturbance becomes too large to keep human/robots still, stepping out will be carried out.

This paper proposes a CoM-based compliance control for standing maintenance of position controlled humanoid robots based on the recognition that CoM control is more direct than ZMP control and the idea of using body compliance control to keep stable in a more natural way. The method proposed integrates virtual model control [12] with admittance control, where the virtual model control is used to calculate the desired virtual force and the admittance control transfers the desired virtual force to position control command. Here 'position controlled humanoid robots' refers to the humanoid robots of which the joints are operating in position mode. The main contributions of this paper are:

- A variable gain virtual model is designed to generate the desired recovery force. It consists of three spring-damper components, the gains of which are adjusted according to the position of CP (Capture Point) [11]. AMPM [13] is employed to derive the constraints of model from the view of GRF. Benefiting from the correspondence between control variables of the virtual model and AMPM, each spring-damper component has a clear descriptor of GRF.
- An admittance controller is introduced to modulate the expected recovery force on position controlled humanoid robots. It takes the virtual model designed as the ideal impedance and then gets the expected CoM position and body attitude by an AMPM-based integrator, with which position control commands of joints can be calculated.

Experiments of exerting external force disturbance to the robot and changing the slope of the ground demonstrate the effectiveness of the proposed method which makes the position controlled humanoid robot owns the performance similar to that of force controlled robots without any mechanical change.

Remainder of the paper is organized as follows. Section II discusses recent research progress on humanoid balance maintenance against external disturbance. Section III describes the AMPM-based variable gain virtual model. Section IV explains how the admittance controller achieves the ideal impedance defined by the virtual model. Section V shows the confirmatory experiments and discusses their results. Section

*This work is supported by the National Nature Science Foundation of China (Grant No. 61075078), the Natural Science Foundation of Zhejiang Province (Grant No. LQ12F03009) and the Innovation Team of Advanced Technology of Zhejiang Province (Grant No. 2009R50014).

[1]The authors are all with the State Key Laboratory of Industrial Control and Technology, Zhejiang University, Hangzhou, P. R. China. Rong Xiong is the corresponding author. rxiong@iipc.zju.edu.cn

VI summarizes our works and concludes the paper.

II. RELATED WORK

Some researchers applied ZMP control for stable stepping, walking or running of humanoid robots. This kind of strategy is mainly based on the ZMP criteria [14], that the robot keeps stable if and only if its ZMP locates in the support polygon. K. Yokoi et al. [4] proposed a ZMP damping controller and a foot adjusting strategy to maintain the walking stability of HRP-1S on uneven grounds. J. Kim et al. [5] gave an integrated balance scheme that included a real-time ZMP compensation in the single support phase, a damping control of ankle joint, and a landing position control based on the angular velocity of the torso. This scheme is validated by KHR-2's stable dynamic walking. T. Takenaka [7] introduced a ground reaction force control method and an extended ZMP model control method which used horizontal and rotational acceleration of the upper body and changed step duration to generate moments to handle disturbance too large to be handled by ground reaction force control. By integrating the two methods, ASIMO achieved both balance recovery from external disturbances and stable running.

The basic idea of real-time ZMP correction is calculating the new reference ZMP according to the ZMP feedback from force/torque sensors. However, the measurement of ZMP feedback, which reflects the effect of external disturbance, lags behind the change of the actual CoM and body's posture angle. The sensing delay results in a slow response of the controller and may cause the system oscillating. For the position controlled humanoid robots, due to the execution error, large GRF may be generated when the swing leg lands on the ground. The slow response makes it difficult for ZMP controller to deal with this impact. Thus, as the methods mentioned above, it needs to be integrated with other strategies, such as a damping control of ankle joint. R. Tajima et al. [8] proposed a compliance control for toe, ankle, and knee joints by setting the joint with low gain to follow external torque. A feedback controller was also presented in order to remove the following errors respect to the original CoM trajectory due to the compliance motion of joints. Some mechanical modifications were also introduced. Z. Li et al. [3] employed physical elasticity to reduce and absorb instantaneous impacts with an active compliance control for standing maintenance. The experiments conducted on the compliant humanoid robot COMAN showed that the robot can recovery from external impacts and adapt to slopes and uneven grounds.

In consideration of the position mode's limitation, force controlled humanoid robots that use the force control mode to actuate its joints were developed and corresponding balance control methods were proposed. J. Pratt et al. [15] introduced the capturability-based analysis and control for step location adjustment, the effect of which is demonstrated on the force controlled humanoid robot M2V2. J. Englsberger et al. [6] described the CP tracking and CP end-of-step controller to realize the DLR Biped stable standing and dynamic walking under external disturbances. B. Stephens [1] proposed CoP Balancing, CMP Balancing and Stepping strategies for balance to resist varying strength push on the Sacros Humanoid Robot. S. Hyon at el. [2] presented a balance controller that transforms the required ground reaction force into full-body joint torques, which makes the compliant humanoid robot CB stand stably under the disturbance from unknown external forces.

Compared with above methods, we focus on standing maintenance problem and adopt the force compliance idea to control the CoM of the position controlled humanoid robot, which enables the robot response quickly and show good compliance and stability to unknown external disturbance.

III. AMPM-BASED VIRTUAL MODEL

A. Design Idea

Virtual Model Control uses virtual mechanical components to generate reference actuator torques or force[12]. In this work, we design an AMPM-based variable gain virtual model to generate desired recovery force which takes GRF constraints into account. The model designed for standing maintenance with a compliant pose control consists of three spring-damper components and the gain of the model will change with the varying location of the CP.

The essence of any motion control or balance control method is to regulate GRF. It means the force or torque command generated by the Virtual Model Control should eventually provided by the GRF. To simplify the control problem, we separate the whole balance control problem into two parts, the control in the longitudinal direction and that in the lateral direction respectively, and take the control in the longitudinal direction as example. Thus any GRF can be determined uniquely by a horizontal force, a vertical force, and an angular torque relative to the CoM. AMPM simplifies the humanoid robot as a momentum-included mass component with a massless leg connecting the CoM and CoP (Center of Pressure). The horizontal and vertical accelerations of the CoM and the torque exerted on the CoM are corresponding with the three components of the GRF respectively. Based on the relationship above, different with the virtual models defined in [16], we propose an AMPM-based virtual model. It consists of three spring-damper components, each of which is correspondent with a component of GRF. Using the correspondence between AMPM and GRF, constraints of the model can be easily determined.

According to the concept of the CP/CR (Capture Region) introduced by Jerry Pratt [11], we can get the premise of standing maintenance algorithm: an intersection region must be shared between the CP/CR and the support polygon. This means the generated virtual force should prevent the robot's feet from rolling over or slipping off. In order to ensure this, constraints must be applied to the virtual force and adapt to the status of robot. Here, we introduce a variable gain into the virtual force model, which is a function of CP. CP is a favorable norm to assess the stability of robots in the view of the premise of standing maintenance. When the CP locates near to the center of the support area, the horizontal

component of the GRF needs to be large enough so that the robot can recover fast, while when the CP is close to the edge of the support area, the horizontal component of the GRF should be limited to meet the constraints of the GRF. In other words, CP has a closely relationship to the permissible GRF. In addition, because the CP represents both the location and velocity of the CoM, it has a phase advance to the CoM. When the robot is recovering from disturbances towards the equilibrium position, the CP will move to the center of support area before the CoM arrived. This means an earlier deceleration can be presented by using the CP as the argument of the variable gain function than that by using the CoM.

B. AMPM-based Force Analysis

AMPM is an extension of IPM (Inverted Pendulum Model) by expanding the mass point to a momentum included mass component [13]. Based on the AMPM, the force and torque acting on the robot are shown as Fig. 1(a). The GRF F_g is orthogonally decomposed into horizontal component F_x and vertical component F_z. If only considering the motion of the CoM, the AMPM is equivalent to the IPM which is shown as Fig. 1(b). The virtual leg connecting the virtual CoP and the CoM is parallel to the direction of F_g. Fig. 2 illustrates the definition of the coordinate frame, which takes the projection of CoM's equilibrium position on the ground as the origin, and the important parameters of the dynamic model. Table I explains the symbols in Fig. 2.

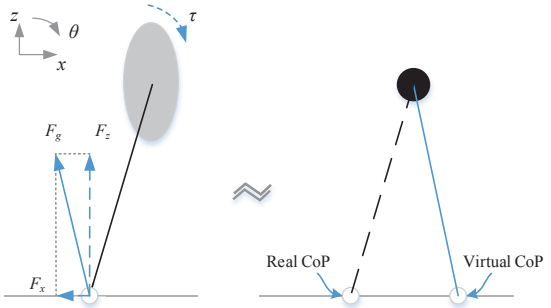

Fig. 1. AMPM-based force analysis and its equivalent model. (a) AMPM-based force analysis; (b) equivalent model describing the CoM movement

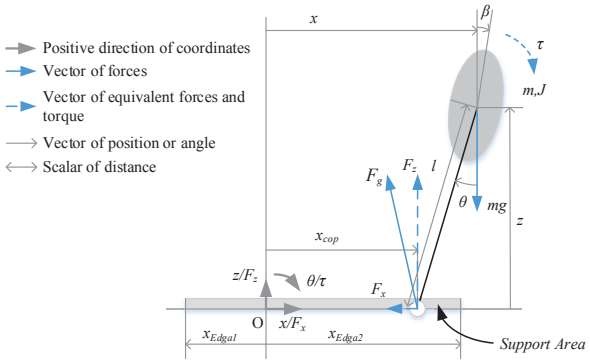

Fig. 2. Parameters of the dynamic model

From the force point of view, the dynamic equations can be written as follow:

$$m\ddot{x} = F_x \tag{1}$$

$$m\ddot{z} = F_z - mg \tag{2}$$

$$J\ddot{\beta} = \tau = (F_z \sin\theta - F_x \cos\theta)l \tag{3}$$

TABLE I
DEFINITIONS OF THE SYMBOLS IN FIG. 2

Symbol	Definition
m	total mass
J	rotational moment to CoM
x_{Edge1}	back edge of support area
x_{Edge2}	font edge of support area
β	body attitude angle
θ	rotation angle of virtual leg
x	horizontal position of CoM
z	vertical position of CoM
x_{cop}	horizontal position of CoP
l	length of virtual leg
F_g	ground reaction force
F_x	horizontal component of GRF
F_z	vertical component of GRF
τ	torque of GRF relative to CoM
g	acceleration of gravity

C. Derivation of the Virtual Model

The proposed virtual model for standing maintenance control is shown as Fig. 3(a). The virtual model can be decomposed into three spring-damper components in rotational, vertical and horizontal directions respectively, which are shown as Fig. 3(b), 3(c) and 3(d), in sequence.

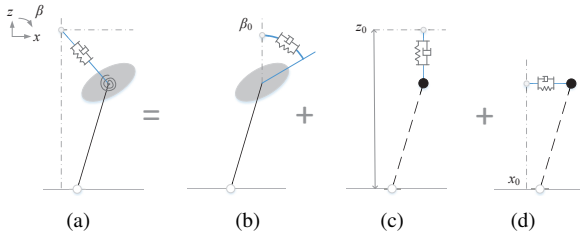

Fig. 3. Proposed virtual model and its three components. (a) overview of the virtual model; (b) the sprint-damping component in rotational(β) direction; (c) the spring-damping component in vertical(z) dircetion; (d) the spring-damping component in horizontal(x) direction

As the discussion in Section III.*A*, the gains of the three components are defined as the function of CP, the output of which should decrease when the distance from the CP to the origin increases. Thus, we use the Gaussian Function as the variable gain function. Taking x direction as an example, we have:

$$g(x_{cp}, a, b, D) = ae^{-x_{cp}^2/b^2} + D \tag{4}$$

where x_{cp} is the position of the CP in x direction, $x_{cp} = x + \dot{x}\sqrt{\frac{z}{g}}$, a, b are parameters of the Gaussian Function, which determines the peak value of gain and the width of high gain area respectively, D is an offset, which settles the base value of gain, $g(x_{cp}, a, b, D) \in (0, 1]$.

For each spring-damper component, we have

$$f(p, p_0, k, c) = -k(p - p_0) - c\dot{p} \tag{5}$$

where p is the current position of the spring-damper end-point, p_0 is the equilibrium position of the spring-damper

endpoint, $\dot{p}$ is the velocity of the spring-damper endpoint, k is the spring constant, c is the damping coefficient.

Then, by combining the variable gain function, we get the ideal output without the GRF constraints:

$$\tau' = g(x_{cp}, a_1, b_1, D_1) \cdot f(\beta, \beta_0, k_1, c_1) \tag{6}$$

$$\ddot{z}' = g(x_{cp}, a_2, b_2, D_2) \cdot f(z, z_0, k_2, c_2) \tag{7}$$

$$\ddot{x}' = g(x_{cp}, a_3, b_3, D_3) \cdot f(x, x_0, k_3, c_3) \tag{8}$$

where $\tau', \ddot{z}', \ddot{x}'$ are ideal rotational torque of the body, vertical and horizontal accelerations of the CoM, a_1, b_1, D_1 are gain function parameters in β direction, a_2, b_2, D_2 are gain function parameters in z direction, a_3, b_3, D_3 are gain function parameters in x direction, β_0, z_0, x_0 are expected positions in β, z, x directions, k_1, k_2, k_3 are spring constants , c_1, c_2, c_3 are damping coefficients.

The virtual model outputs should satisfy the following robot's mechanical and GRF constraints:

$$\tau \in [\tau_{min}, \tau_{max}] \tag{9}$$

$$\ddot{z} \in [\ddot{z}_{min}, \ddot{z}_{max}] \tag{10}$$

$$x_{cop} \in [x_{Edge1}, x_{Edge2}] \tag{11}$$

where $\tau, \ddot{z}, x_{cop}$ are body rotational torque, vertical acceleration of the CoM and position of the CoP, τ_{min}, τ_{max} are minimum and maximum body torque, $\ddot{z}_{min}, \ddot{z}_{max}$ are minimum and maximum vertical acceleration of the CoM.

Using the dynamic equations (1)∼(3) of the AMPM model and $\sin\theta = \frac{x - x_{cop}}{l}, \cos\theta = \frac{z}{l}, l = \sqrt{(x - x_{cop})^2 + z^2}$, we get:

$$x_{cop} = x - \frac{\ddot{x}}{g + \ddot{z}} z - \frac{\tau}{m(g + \ddot{z})} \tag{12}$$

Substituting (12) into the constraint (11), we get the constraint of the horizontal acceleration of the CoM $\ddot{x}$:

$$\ddot{x} \in [\ddot{x}_{min}, \ddot{x}_{max}] \tag{13}$$

where

$$\ddot{x}_{min} = (x - x_{Edge2} - \frac{\tau^d}{m(g + \ddot{z}^d)}) \cdot (\frac{g + \ddot{z}^d}{z}) \tag{14}$$

$$\ddot{x}_{max} = (x - x_{Edge1} - \frac{\tau^d}{m(g + \ddot{z}^d)}) \cdot (\frac{g + \ddot{z}^d}{z}) \tag{15}$$

Using τ' and $\ddot{z}'$ from (6)∼(7) to replace τ and $\ddot{z}$ in the constraints (9)∼(10), we can get the desired body torque τ^d, vertical acceleration of the CoM $\ddot{z}^d$. Using τ^d and $\ddot{z}^d$ to replace τ and $\ddot{z}$ in (14)∼(15) and using $\ddot{x}'$ from (8) to replace $\ddot{x}$ in the constraint (13), we can get the desired horizontal acceleration of the CoM $\ddot{x}^d$. So, the desired outputs of the virtual model:

$$\tau^d = \begin{cases} \tau_{min} & \tau' < \tau_{min} \\ \tau' & \tau_{min} \le \tau' \le \tau_{max} \\ \tau_{max} & \tau_{max} < \tau' \end{cases} \tag{16}$$

$$F_z^d = m\ddot{z}^d + mg = \begin{cases} m\ddot{z}_{min} + mg & \ddot{z}' < \ddot{z}_{min} \\ m\ddot{z}' + mg & \ddot{z}_{min} \le \ddot{z}' \le \ddot{z}_{max} \\ m\ddot{z}_{max} + mg & \ddot{z}_{max} < \ddot{z}' \end{cases} \tag{17}$$

$$F_x^d = m\ddot{x}^d = \begin{cases} m\ddot{x}_{min} & \ddot{x}' < \ddot{x}_{min} \\ m\ddot{x}' & \ddot{x}_{min} \le \ddot{x}' \le \ddot{x}_{max} \\ m\ddot{x}_max & \ddot{x}_{max} < \ddot{x}' \end{cases} \tag{18}$$

where F_z^d, F_x^d are desired virtual forces in vertical and horizontal direction respectively.

IV. AMPM-BASED ADMITTANCE CONTROL

A. Controller Structure

The virtual model describes the desired impedance of the standing maintenance control. There are two approaches to realize the desired impedance: Impedance Control and Admittance Control, which are distinguished by the input and output variables. The Impedance Controller accepts force inputs and determines its motion in response, while the Admittance Controller accepts motion inputs and determines its force in response[17]. A position controlled humanoid robot is driven by joints position commands, which means the desired impedance can be implemented in the admittance form. We adopt an AMPM-based integrator to get the desired angle of the body posture and position of the CoM.

The overview of the controller is shown as Fig. 4, where the position controlled system includes the robot system and the forward and backward kinematics calculation. In this structure, the inputs and outputs of the controller are the same variables. We can easily determine whether the external disturbance happened by comparing the actual and previously desired posture angle and CoM, which helps to achieve a fast response to external disturbances and realize precise control over the impedance.

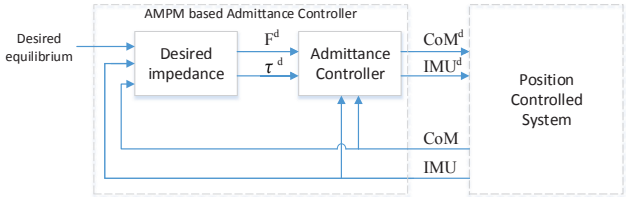

Fig. 4. Overview of the controller

B. Calculation of Desired Impedance

The controller use the proposed virtual model control to get the desired impedance. Without external disturbance, there are only two forces applied on the robots. One is the GRF and the other one is the gravity. The gravity of the robot has constant magnitude and direction, and zero torque respect to the CoM. Therefore, when the external disturbance is absent, the motion of robots can be determine by the GRF, which means we can control the GRF to get our desired impedance. Based on the definition of the three spring-damper components, we can get the desired body torque τ, vertical force F_z and horizontal force F_x which are presented as (16)∼(18). The desired torque/forces response conform the desired impedance.

C. Desired Impedance Implement

We use an AMPM-based integrator to implement the desired impedance. The integrator accepts the desired torque/forces from the virtual model as input and solves for

the desired position of the CoM and the posture angle of the body as output. Based on the AMPM, we can get expression:

$$\begin{bmatrix} \beta^d \\ z^d \\ x^d \end{bmatrix} = \int_0^T \left(\int_0^T \begin{bmatrix} \ddot{\beta}^d \\ \ddot{z}^d \\ \ddot{x}^d \end{bmatrix} dt + \begin{bmatrix} \dot{\beta} \\ \dot{z} \\ \dot{x} \end{bmatrix} \right) dt + \begin{bmatrix} \beta \\ z \\ x \end{bmatrix} \tag{19}$$

where β^d is desired attitude angle, z^d, x^d are desired vertical and horizontal position, and

$$\begin{bmatrix} \ddot{\beta}^d \\ \ddot{z}^d \\ \ddot{x}^d \end{bmatrix} = \begin{bmatrix} \frac{F_x^d}{m} \\ \frac{F_z^d}{m} - g \\ \frac{\tau^d}{J} \end{bmatrix} \tag{20}$$

V. EXPERIMENTAL RESULTS

A. Humanoid Platform

To test our algorithm, experiments are conducted on the humanoid robot 'Kong' as shown in Fig. 5(a). The robot is 161 *cm* in height with a total mass of 53 *kg* and 14 DOFs (Degree of Freedom), where 6 DOF in each leg and 2 DOF in the waist. The main constrains and parameters of our algorithm are listed in Table II.

An IMU (Inertia Measurement Unit) is mounted at the middle of the waist to measure the body posture. Each joint is equipped with an encoder to read its angle. A 6-axis force/torque sensor is installed between the ankle and the foot in each leg to record the real GRF and torque for data analysis. In order to measure the strength of the disturbances, we installed a same force/torque sensor at the endpoint of the disturbance device (shown as Fig. 5(b)). The measurement of disturbance is only used for data comparison. It is totally unknown to the controller.

TABLE II

MAIN CONSTRAINS AND CONTROL SETTINGS

m	$\approx 53kg$	β_0	$= 0.000rad$	τ_{min}	$= -50rad/s^2$
J	$\approx 0.3kg \cdot m^2$	z_0	$= 0.815m$	τ_{max}	$= 50rad/s^2$
x_{Edge1}	$= -0.10m$	x_0	$= 0.000m$	$\ddot{z}_{min}$	$= -2m/s^2$
x_{Edge2}	$= 0.13m$			$\ddot{z}_{max}$	$= 2m/s^2$
				T	$= 20ms$
				T_s	$= 10ms$

T is the control period. T_s is the sampling period.

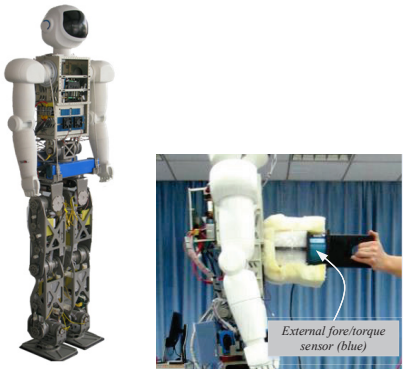

(a) (b)

Fig. 5. Humanoid platform and disturbance device. (a) The humanoid 'Kong'; (b) The disturbance device with a force/torque sensor

B. Balance under Unknown Push

Balance experiment under unknown push was conducted to demonstrate the compliance and stability of proposed standing maintenance controller under push disturbances. The values of the virtual model parameters, which were manually modified based on their definition and effect, are listed in Table III.

Fig. 6 is the impact disturbances applied on the humanoid. Using the body attitude angle and joint angles, the movement of the CoM, the angle of feet, as well as the position of the CP are calculated. Fig. 7 shows the horizontal position and velocity of the CoM and the position of the CP. The rotation angle of the feet is shown in Fig. 8. Using these information, the virtual model calculates the desired GRF which satisfies the constraints. The AMPM-based integrator transforms the virtual force into the motion of the CoM and the body attitude angle. The real GRF and torques are measured by the 6-axis force/torque sensors equipped at the robots feet and transformed into world coordinate frame according to the calculated feet angle. Fig. 9 compares the desired horizontal GRF F_x^d and the measured horizontal GRF F_x^m. Fig. 10 compares the desired vertical GRF F_z^d and the measured vertical GRF F_z^m. Fig. 11 compares the desired body torque τ^d and the measured body torque τ^m. Fig. 12 shows the humanoid recovery after the 4^{th} impact disturbance.

The comparison of the desired GRF/torque and the measured GRF/torque in three directions proves that the desired impedance is well realized. By looking into the data we collected, we discover that, when the robot suffered from external disturbances or had a relatively obvious foot angle, the error between desired and measured force/torque would be enlarged. It is easy to understand that the external disturbances applied on the robot causing the following error of the desired force because the desired impedance calculation assumed only GRF and gravity applied on the robot. There are two reasonable explanation for the following error occurred when the rotation angle of foot is relatively large. One is the underactuation between feet and ground,which produces an uncontrollable torque on the feet. Because the force/torque sensors are installed between feet and ankles, this additional torque is unmeasurable. When the rotation angle of the foot is relatively large, its rotational velocity is also relatively large, which enlarges the following error. Another explanation is the error of foot angle measurement leads to the error of gravity compensation and coordination transformation which finally causes the following error of desired force.

TABLE III

PARAMETERS' VALUE OF THE VIRTUAL MODEL WITH VARIABLE GAIN FOR THE EXPERIMENT OF EXERTING PUSH DISTURBANCE

a_1	=	0.87	a_2	=	0.67	a_3	=	0.87
b_1	=	0.03	b_2	=	0.07	b_3	=	0.03
D_1	=	0.13	D_2	=	0.33	D_3	=	0.13
k_1	=	3.47	k_2	=	12.00	k_3	=	4.22
c_1	=	5.79	c_2	=	18.00	c_3	=	8.44

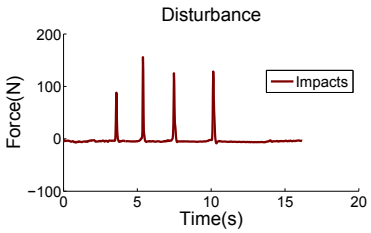

Fig. 6. The impact disturbances

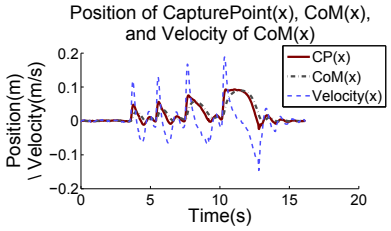

Fig. 7. The position and velocity of the CoM in horizontal direction and the position of the CP

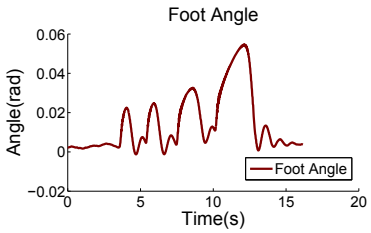

Fig. 8. The angle between feet and ground

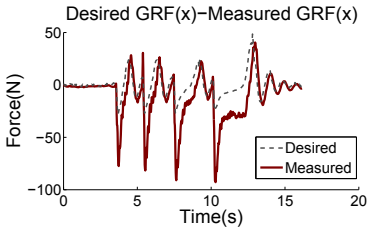

Fig. 9. The desired and measured GRF horizontal components

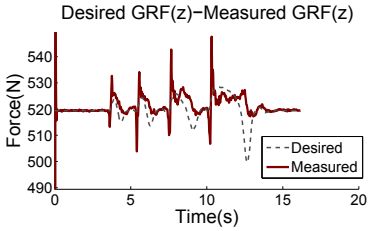

Fig. 10. The desired and measured GRF vertical components

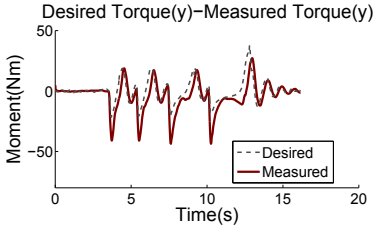

Fig. 11. The desired and measured GRF torque relative to the CoM

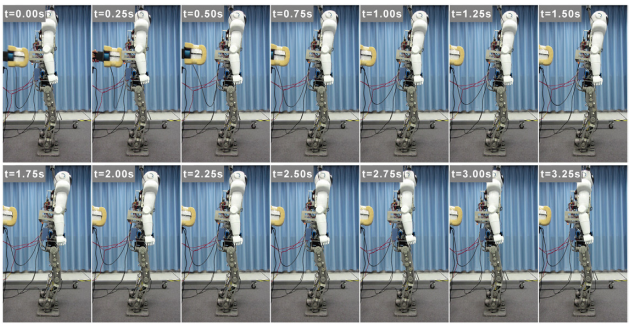

Fig. 12. The humanoid recovery of the 4^{th} impact disturbance

C. Comparison between the Variable and Fixed Gain

In Section III.*A*, we have discussed why a variable gain is needed. The advantage of the variable gain is to decrease the possibility of the feet rolling over. Because of the underactuation between feet and ground, feet rolling will cause undesired torque at the contact point of the feet and the ground and leads to the following error of the desired GRF. Serious feet rolling may lead to oscillation of the robot and the divergence of the controller.

To evaluate the effectiveness of the variable gain, comparison experiment using fixed gain is conducted. Three appropriate fixed gains are selected based on the range of the former variable gains. The values of the spring constant and damping coefficient are listed in Table IV. Fig. 13 is the impact disturbances applied on the robot. Fig. 14 shows the horizontal position and velocity of the CoM and the position of the CP. The rotation angle of the feet is shown in Fig. 15. Fig. 16 compares the desired horizontal GRF F_x^d and the measured horizontal GRF F_x^m. Fig. 17 compares the desired vertical GRF F_z^d and the measured vertical GRF F_z^m. Fig. 18 compares the desired body torque τ^d and the measured body torque τ^m. Under similar strength impacts, like last impact in Fig. 6 and penultimate impact in Fig. 13, there is smaller foot angle maximum during recovery when use the variable gain than that of the fix gain. Comparing the foot angle curve of these two impacts, we can figure out that the impact response decay ratio of variable gain system, about 5:1, is significantly larger than that of fixed gain system, about 3:1, which means a better stability of robot. At the last impact, the robot using fixed gain virtual model tends to diverge. As expected, the result of experiment demonstrated the variable gain bring a stabler performance of impact disturbance recovery. It's because the variable gain utilizes the interrelation of CP-GRF and CP-CoM described in Section III.*A*.

TABLE IV

PARAMETERS' VALUES OF THE VIRTUAL MODEL WITH FIXED GAIN

k_1	=	1.58	k_2	=	12.00	k_3	= 1.92
c_1	=	2.64	c_2	=	18.00	c_3	= 3.85

D. Balance on Changing Slope

The proposed controller is also suitable for robot standing maintenance control when the ground is not totally horizontal and changing with time. The appropriate values of the virtual

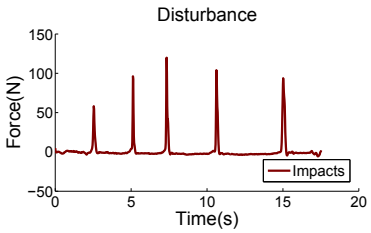

Fig. 13. The impact disturbances

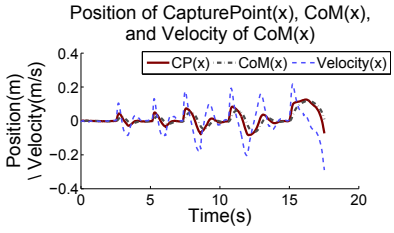

Fig. 14. The position and velocity of the CoM in horizontal direction and the position of the CP

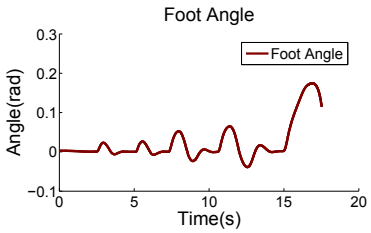

Fig. 15. The angle between feet and ground

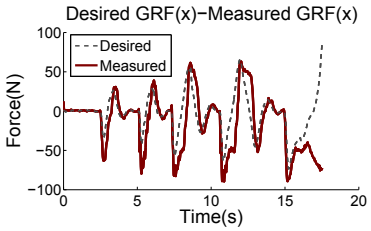

Fig. 16. The desired and measured GRF horizontal components

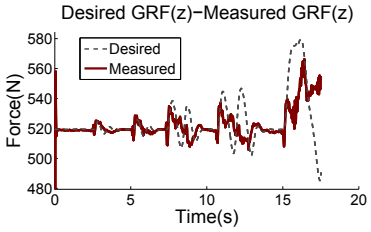

Fig. 17. The desired and measured GRF vertical components

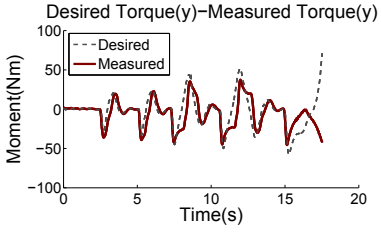

Fig. 18. The desired and measured GRF torque relative to the CoM

model parameters are listed in Table V. Fig. 19 shows the horizontal position and velocity of the CoM and the position of the CP. The rotation angle of the feet is shown in Fig. 20. Fig. 21 compares the desired horizontal GRF F_x^d and the measured horizontal GRF F_x^m. Fig. 22 compares the desired vertical GRF F_z^d and the measured vertical GRF F_z^m. Fig. 23 compares the desired body torque τ^d and the measured body torque τ^m. Fig. 24(a) shows the process of the ground slope increasing from zero degree and Fig. 24(b) shows the process of the ground slope decreasing to zero degree. We discover that in Fig. 21, 22 and 23, curves are oscillatory. These oscillations are mostly caused by the oscillation of disturbance force/torque. As the Fig. 24(a) and 24(b) shown, the operator cannot keep slope at a certain angle or change it at a certain velocity. The high frequency disturbance lead the oscillatory of measured GRF/torque and the error of desired force/torque following. However, from the data of CoM and CP, we still can draw the conclusion that the proposed method is effective in balancing on changing slope.

TABLE V

PARAMETERS' SETTING OF THE VIRTUAL MODEL WITH VARIABLE GAIN FOR EXPERIMENT OF CHANGING GROUND SLOPE

a_1	=	0.68	a_2	=	0.67	a_3	=	0.68
b_1	=	0.04	b_2	=	0.07	b_3	=	0.07
D_1	=	0.32	D_2	=	0.33	D_3	=	0.32
k_1	=	1.24	k_2	=	12.00	k_3	=	4.22
c_1	=	3.72	c_2	=	18.00	c_3	=	12.66

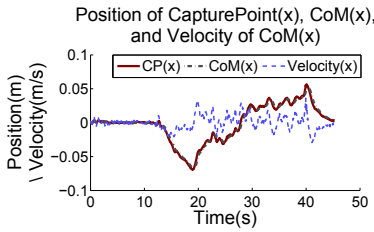

Fig. 19. The position and velocity of the CoM in horizontal direction and the position of the CP

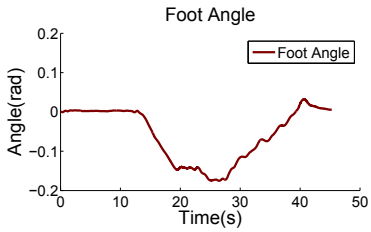

Fig. 20. The angle between feet and ground

VI. CONCLUSIONS

In this paper, we present a standing maintenance control algorithm for humanoid robots, which is composed of an AMPM-based virtual model with variable gain and an AMPM-based admittance controller. The virtual model describes the desired impedance with GRF constraints. The application of the variable gain helps greatly to decrease the

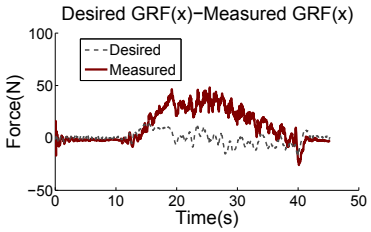

Fig. 21. The desired and measured GRF horizontal components

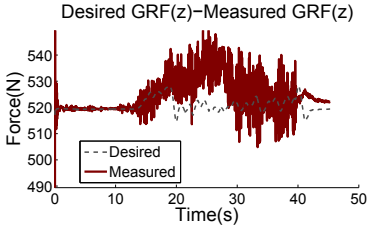

Fig. 22. The desired and measured GRF vertical components

possibility of feet rolling over and avoid the divergence of the controller. Experiments conducted on the real humanoid robot 'Kong' validate the effectiveness of our method.

Next we will extend the proposed algorithm for stable walking and make the parameters of the virtual model be self-adaptive to the diverse tasks with optimal performance.

REFERENCES

[1] B. Stephens, "Humanoid push recovery," in *Humanoid Robots, 2007 7th IEEE-RAS International Conference on*, ser. Humanoid Robots, 2007 7th IEEE-RAS International Conference on. IEEE, 2007, pp. 589–595.

[2] S.-H. Hyon, J. G. Hale, and G. Cheng, "Full-body compliant human-humanoid interaction: balancing in the presence of unknown external forces," *Robotics, IEEE Transactions on*, vol. 23, no. 5, pp. 884–898, 2007.

[3] Z. Li, N. G. Tsagarakis, and D. G. Caldwell, "A passivity based admittance control for stabilizing the compliant humanoid coman," in *Humanoid Robots (Humanoids), 2012 12th IEEE-RAS International Conference on*. IEEE, 2012, pp. 43–49.

[4] K. Yokoi, F. Kanehiro, K. Kaneko, S. Kajita, K. Fujiwara, and H. Hirukawa, "Experimental study of humanoid robot hrp-1s," *The International Journal of Robotics Research*, vol. 23, no. 4-5, pp. 351–362, 2004.

[5] J.-Y. Kim, I.-W. Park, and J.-H. Oh, "Experimental realization of dynamic walking of the biped humanoid robot khr-2 using zero moment point feedback and inertial measurement," *Advanced Robotics*, vol. 20, no. 6, pp. 707–736, 2006.

[6] J. Englsberger, C. Ott, M. A. Roa, A. Albu-Schaffer, and G. Hirzinger, "Bipedal walking control based on capture point dynamics," in *Intelligent Robots and Systems (IROS), 2011 IEEE/RSJ International Conference on*, ser. Intelligent Robots and Systems (IROS), 2011 IEEE/RSJ International Conference on. IEEE, 2011, pp. 4420–4427.

[7] T. Takenaka, T. Matsumoto, T. Yoshiike, T. Hasegawa, S. Shirokura, H. Kaneko, and A. Orita, "Real time motion generation and control for biped robot- 4^{th} report: Integrated balance control," in *Intelligent Robots and Systems, 2009. IROS 2009. IEEE/RSJ International Conference on*, ser. Intelligent Robots and Systems, 2009. IROS 2009. IEEE/RSJ International Conference on. IEEE, 2009, pp. 1601–1608.

[8] R. Tajima, D. Honda, and K. Suga, "Fast running experiments involving a humanoid robot," in *Robotics and Automation, 2009. ICRA'09. IEEE International Conference on*, ser. Robotics and Automation, 2009. ICRA'09. IEEE International Conference on. IEEE, 2009, pp. 1571–1576.

[9] R. Tajima and K. Suga, "Motion having a flight phase: Experiments involving a one-legged robot," in *Intelligent Robots and Systems, 2006 IEEE/RSJ International Conference on*, ser. Intelligent Robots and Systems, 2006 IEEE/RSJ International Conference on. IEEE, 2006, pp. 1726–1731.

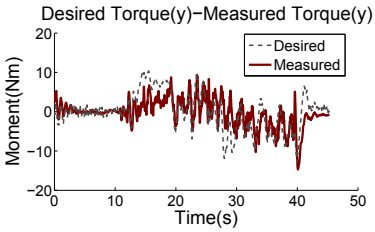

Fig. 23. The desired and measured GRF torque relative to the CoM

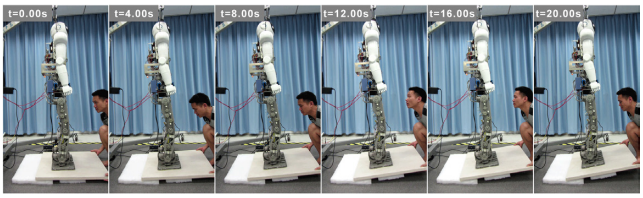

(a) The process of the ground slope increasing from zero degree

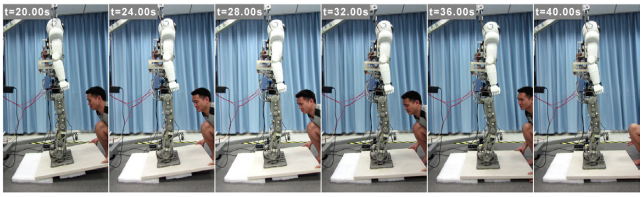

(b) The process of the ground slope decreasing to zero degree

Fig. 24. Snapshots of balancing under slope varying

[10] R. Xiong, Y. Sun, Q. Zhu, J. Wu, and J. Chu, "Impedance control and its effects on a humanoid robot playing table tennis," *Int J Adv Robotic Sy*, vol. 9, no. 178, 2012.

[11] J. Pratt, J. Carff, S. Drakunov, and A. Goswami, "Capture point: A step toward humanoid push recovery," in *Humanoid Robots, 2006 6th IEEE-RAS International Conference on*, ser. Humanoid Robots, 2006 6th IEEE-RAS International Conference on. IEEE, 2006, pp. 200–207.

[12] J. Pratt, P. Dilworth, and G. Pratt, "Virtual model control of a bipedal walking robot," in *Robotics and Automation, 1997. Proceedings., 1997 IEEE International Conference on*, ser. Robotics and Automation, 1997. Proceedings., 1997 IEEE International Conference on, vol. 1. IEEE, 1997, pp. 193–198.

[13] S. Kudoh and T. Komura, "c^2 continuous gait-pattern generation for biped robots," in *Intelligent Robots and Systems, 2003.(IROS 2003). Proceedings. 2003 IEEE/RSJ International Conference on*, ser. Intelligent Robots and Systems, 2003.(IROS 2003). Proceedings. 2003 IEEE/RSJ International Conference on, vol. 2. IEEE, 2003, pp. 1135–1140.

[14] M. Vukobratovi and J. Stepanenko, "On the stability of anthropomorphic systems," *Mathematical Biosciences*, vol. 15, no. 1, pp. 1–37, 1972.

[15] J. Pratt, T. Koolen, T. De Boer, J. Rebula, S. Cotton, J. Carff, M. Johnson, and P. Neuhaus, "Capturability-based analysis and control of legged locomotion, part 2: Application to m2v2, a lower-body humanoid," *The International Journal of Robotics Research*, vol. 31, no. 10, pp. 1117–1133, 2012.

[16] R. Ekkelenkamp, P. Veltink, S. Stramigioli, and H. van der Kooij, "Evaluation of a virtual model control for the selective support of gait functions using an exoskeleton," in *Rehabilitation Robotics, 2007. ICORR 2007. IEEE 10th International Conference on*, ser. Rehabilitation Robotics, 2007. ICORR 2007. IEEE 10th International Conference on. IEEE, 2007, pp. 693–699.

[17] N. Hogan, "Impedance control: An approach to manipulation," in *American Control Conference, 1984*, ser. American Control Conference, 1984. IEEE, 1984, pp. 304–313.